

PERIODIC VISCOUS FLOW: A BENCH-MARK PROBLEM

I. S. GOLDBERG

Engineering and Physics Departments, St. Mary's University, San Antonio, TX 78284, U.S.A.

AND

G. F. CAREY, R. McLAY AND L. PHINNEY

Aerospace Engineering and Engineering Mechanics Department, The University of Texas at Austin, Austin, TX 78712, U.S.A.

SUMMARY

A double-transform technique provides a semi-analytic solution in the form of a series expansion for unsteady axisymmetric Stokes flow in the entrance region of a semi-infinite rigid cylindrical tube. This in turn offers an appropriate bench-mark problem for evaluating the quality of numerical approximations. To illustrate this, periodic axial flow in a circular cylinder is considered. Some aspects of the bench-mark problem that are of interest include the reverse flow in the wall layers, the accuracy of the approximate method in different flow regimes and the mesh grading. This bench-mark problem and the numerical study provide some insight into practical issues pertinent to the approximate solution of unsteady and periodic flows.

KEY WORDS Periodic Unsteady Viscous flow Finite elements

INTRODUCTION

Numerical approximation of viscous flow problems presents a viable approach for analysis of complex flows in engineering and an important adjunct to experimental and analytical studies. Finite difference and finite element methods have been extensively developed for these and other flow problems and are now in wide use. New variants of the methods are developed periodically and must be tested to ascertain if they offer an improvement on the existing technology. Moreover, as new classes of problems are considered with existing techniques, certain basic questions such as adequacy of the grid and time integration procedure must be addressed if reliable simulations are to be made.

Bench-mark test problems comprise an important component in the evaluation of approximate methods. There are a few well known solutions to viscous flow problems such as those classical solutions for fully developed flows in channels and pipes¹ and the recently obtained solutions for steady entrance flow in pipes.^{2,3} For unsteady and periodic flows there appear to be very few analytic results that offer a good bench-mark for testing the methods or evaluating a new class of problems. The present study is directed to the development of a bench-mark analytic solution for unsteady periodic flows and the associated numerical experiments using a finite element Galerkin formulation for Stokes flow.

Transform techniques were utilized in a previous study³ to obtain a product-series analytic solution for unsteady axisymmetric Stokes flow of an incompressible Newtonian fluid in the

entrance region (and beyond) in a semi-infinite rigid cylindrical tube. In the following discussion this bench-mark problem is briefly described and the analytical results are summarized. We give sufficient details for the general construction to be understood and tabulated results for use in future comparisons. A Galerkin finite element model is then introduced to construct an approximate formulation. Numerical comparison studies of the finite element and analytic solutions are given to assess the quality of the approximate method near the entrance region, in the reverse flow for the wall layer and in other flow regimes.

PROBLEM STATEMENT

Under the stated assumption, the dimensionless time-dependent Stokes equations governing axisymmetric viscous flow in cylindrical co-ordinates reduce to

$$\frac{\partial U}{\partial T} + \frac{\partial P}{\partial Z} - \left(\frac{\partial^2 U}{\partial Z^2} + \frac{\partial^2 U}{\partial R^2} + \frac{1}{R} \frac{\partial U}{\partial R} \right) = 0, \quad (1)$$

$$\frac{\partial V}{\partial T} + \frac{\partial P}{\partial R} - \left(\frac{\partial^2 V}{\partial Z^2} + \frac{\partial^2 V}{\partial R^2} + \frac{1}{R} \frac{\partial V}{\partial R} - \frac{V}{R^2} \right) = 0, \quad (2)$$

$$\frac{\partial U}{\partial Z} + \frac{\partial V}{\partial R} + \frac{V}{R} = 0, \quad (3)$$

where dimensionless quantities are capitalized:

$$\begin{aligned} U &= u/\bar{u}, & R &= r/a, \\ V &= v/\bar{u}, & Z &= z/a, \\ P &= ap/(\rho v \bar{u}), & T &= vt/a^2. \end{aligned} \quad (4)$$

Here u and v are the axial and radial components of the velocity vector, p is the pressure, ρ and ν are the density and kinematic viscosity of the fluid, a is the radius of the tube, t is time, r and z are the radial and axial co-ordinates and \bar{u} is an appropriate velocity scale factor for the non-dimensionalization. On the surface of the tube no slip applies,

$$U(Z, R, T)|_{R=1} = V(Z, R, T)|_{R=1} = 0, \quad (5)$$

and the time-dependent inlet flow velocity is specified. In the present study the entrance condition for periodic flow in a semi-infinite tube is given in terms of a sinusoidally varying axial velocity component of specified frequency together with zero radial component. That is, at $Z=0$ we have

$$U(Z, R, T)|_{Z=0} = U_0(R) \cos(W_0 T), \quad (6)$$

$$V(Z, R, T)|_{Z=0} = 0 \quad (7)$$

for $0 \leq R \leq 1$, $0 \leq Z < \infty$ and $-\infty < T < \infty$. Since many problems of practical interest deal with entrance flow difficulties, in the present study we have set

$$U_0(R) = \begin{cases} 1 & \text{when } 0 \leq R \leq 0.95, \\ 1 - (R - 0.95)^2 / (1 - 0.95)^2 & \text{when } 0.95 < R \leq 1, \end{cases} \quad (8)$$

so that the axial velocity at the entrance of the tube is uniform except near the walls where it parabolically approaches zero in a small layer region. The analytical results described later have been obtained for general inlet flows and periodic flows with a wide range of frequencies. For

purposes of the present comparison and bench-mark study we select typical frequencies of $W_0 = 30$ and 60 for the numerical calculations, where the flow is above frequencies which are quasi-steady and below frequencies where the assumption of unsteady Stokes flow becomes invalid.

ANALYTICAL RESULTS

The above problem in which two velocity components are specified at $Z = 0$ is referred to as a pure entrance condition problem. In contrast, a problem in which only one component of velocity is specified at the entrance with a second entrance condition specified either in terms of pressure or in terms of a normal component of a velocity gradient is known as a mixed entrance condition problem. The semi-analytic entrance flow solutions of the pure entrance condition problems, presented later in this treatment, are obtained in an indirect manner in which two mixed entrance condition problems are first solved. In each of these mixed problems, one component of entrance velocity is specified to be identical to a component of entrance velocity for the pure entrance condition problem while the second entrance condition is left as an unspecified function to be determined from a correspondence relation.

Both types of mixed entrance condition problems are solved analytically to yield closed-form solutions in series form in which the normal mode expansion coefficients β are given in terms of integrals containing appropriate boundary conditions. A correspondence relation is then developed from which two unspecified boundary functions can be determined so that the two mixed entrance conditions have identical solutions for all Z , R and T . Thus the solution to either mixed entrance condition problem is equal to the solution of the pure entrance condition problem with U and V specified at $Z=0$. The indicated correspondence relation is solved by truncated orthogonal expansions for Fourier transforms or complex amplitudes of the unspecified boundary condition. The truncated expansions ensure that the two mixed entrance condition problems have identical solutions from some finite Z to infinity. The truncated correspondence relation is solved numerically and to this extent only is the result 'semi'-analytical. Note that the correspondence relations are, however, obtained as the analytical solution to mixed entrance condition problems.

The solution consists of a superposition of the developed flow solutions, denoted by U_∞ , V_∞ and P_∞ , together with the entrance flow solutions, denoted by U_1 , V_1 and P_1 .⁴⁻⁶ This superposition may be formally expressed as

$$U = U_\infty + U_1, \quad V = V_\infty + V_1, \quad P = P_\infty + P_1, \quad (9)$$

where P_1 is referred to as an excess entrance pressure.

For the specific choice of entrance conditions given by (6)–(8), the developed flow solutions are^{1,3,4}

$$U_\infty = \text{Re} \left(\frac{0.9671 [J_0(i^{3/2} \sqrt{W_0} R) - J_0(i^{3/2} \sqrt{W_0})] \exp(iW_0 T)}{J_2(i^{3/2} \sqrt{W_0})} \right), \quad (10)$$

$$V_\infty = 0, \quad (11)$$

$$\frac{\partial P_\infty}{\partial Z} = \text{Re} \left(\frac{0.9671 W_0 i J_0(i^{3/2} \sqrt{W_0}) \exp(iW_0 T)}{J_2(i^{3/2} \sqrt{W_0})} \right), \quad (12)$$

where $\text{Re}(\)$ denotes the real part of a complex function, $i = \sqrt{-1}$ and J_0 and J_2 are Bessel functions. The factor 0.9671 is a result of rounding of the entrance profile at the corners. Note

that, from equation (12), P_∞ is independent of R and decreases linearly with Z . The amplitude of the pressure is determined only within an arbitrary additive constant which here is taken for convenience to give a reference value $P_\infty = 0$ at $Z = 1.2$. Numerical results given subsequently are for the dimensionless frequency $W_0 = 30$, in which case equation (12) reduces to

$$\frac{\partial P_\infty}{\partial Z} = -37.50 \cos(30T + 73.2^\circ). \quad (13)$$

The solutions for the entrance flow contributions may be expressed in the form of a normal mode expansion as

$$\begin{bmatrix} U_1(Z, R, T) \\ V_1(Z, R, T) \\ P_1(Z, R, T) \end{bmatrix} = Re \left(\sum_n \frac{\beta_n}{(\partial F / \partial K)} \begin{bmatrix} \phi_U(K, R, W_0) \\ \phi_V(K, R, W_0) \\ \phi_P(K, R, W_0) \end{bmatrix} \exp [i(W_0 T + KZ)] \right) \Bigg|_{W_0=30}^{K=K_n(W_0)}, \quad (14)$$

which are also evaluated in the present case for $W_0 = 30$ with summation over the normal modes corresponding to the roots of the frequency equation with positive imaginary parts. The associated frequency equation is defined as $F(K, W_0) = 0$, where

$$F(K, W_0) = H J_0(iH) J_1(iK) - K J_1(iH) J_0(iK), \quad (15)$$

with $H = \sqrt{iW_0 + K^2}$. The corresponding normal mode eigenfunctions are

$$\phi_U(K, R, W_0) = K J_0(iKR) J_1(iH) - H J_0(iHR) J_1(iK), \quad (16)$$

$$\phi_V(K, R, W_0) = K [J_1(iHR) J_1(iK) - J_1(iH) J_1(iKR)], \quad (17)$$

$$\phi_P(K, R, W_0) = -W_0 J_1(iH) J_0(iKR). \quad (18)$$

Now the normal mode coefficients β_n in the expansion defined by equation (14) can be determined in an indirect manner with the use of a correspondence relationship consisting of a truncated set of integral equations (as explained in Reference 3). This correspondence relation is obtained by equating the expressions for

$$\begin{aligned} \beta_n^1(W_0) = & \frac{2}{W_0} \left(\frac{H^2 - 2K^2}{J_1(iK)} \int_0^1 U_0(\xi) \xi J_0(iK\xi) d\xi + \frac{iK}{J_1(iK)} \int_0^1 G_0(\xi) \xi J_1(iK\xi) d\xi \right. \\ & \left. + \frac{KH}{J_1(iH)} \int_0^1 U_0(\xi) \xi J_0(iH\xi) d\xi - \frac{iK}{J_1(iH)} \int_0^1 G_0(\xi) \xi J_1(iH\xi) d\xi \right) \Bigg|_{K=K_n} \end{aligned} \quad (19)$$

and

$$\begin{aligned} \beta_n^2(W_0) = & -\frac{2i}{W_0} \left(\frac{K}{J_1(iK)} \int_0^1 P_0(\xi) \xi J_0(iK\xi) d\xi - \frac{H}{J_1(iH)} \int_0^1 P_0(\xi) \xi J_0(iH\xi) d\xi \right. \\ & \left. + \frac{W_0}{J_1(iH)} \int_0^1 V_0(\xi) \xi J_1(iH\xi) d\xi \right) \Bigg|_{K=K_n}, \end{aligned} \quad (20)$$

where ξ is a dummy integration variable replacing R . In the above integral expressions the entrance condition $U_0(R)$ is specified by (8) and the entrance condition $V_0(R)$ is specified to equal zero according to (7). G_0 and P_0 are complex phase amplitudes related to the unknown entrance conditions at $Z = 0$ for $\partial V / \partial Z$ and P respectively.

Remark. For the sinusoidal periodic flow considered in this paper, complex exponential functions in time are used. This method is more straightforward than the method used in

Goldberg and Folk,³ where a transform in time is taken for solutions to problems in which the time dependence is of a more general nature.

The unknown entrance conditions P_0 and G_0 can be determined from the solution to the correspondence relation for consistency with the specified entrance conditions U_0 and V_0 . The normal mode coefficients β_n are finally obtained by substituting these results into expressions (19) and (20). Under this condition, $\beta_n = \beta_n^1 = \beta_n^2$.

To facilitate a solution to the correspondence relation, the unknown complex functions P_0 and G_0 are replaced by a series of orthogonal functions with unknown complex coefficients, thereby reducing the correspondence relation to a truncated set of algebraic equations. The integrals in the correspondence relation containing the expression $U_0(R)$ given by equation (19) could not be evaluated in closed form, unlike the situation for the problem given by Goldberg and Folk.³ Consequently, Gaussian quadrature was introduced for the numerical evaluation of these integral expressions. The solutions presented in this paper were obtained with 200 modes contained in the correspondence relations. (However, it should be noted that the series converges rapidly and fewer modes are needed for solutions where $Z > 0.02$.)

For convenience in the presentation of results, the solutions for the velocity components and the excess entrance pressure are expressed in the form

$$U(Z, R, T) = A_u \cos(W_0 T + \theta_u), \tag{21}$$

$$V(Z, R, T) = A_v \cos(W_0 T + \theta_v), \tag{22}$$

$$P_1(Z, R, T) = A_p \cos(W_0 T + \theta_p), \tag{23}$$

where A_u , A_v and A_p represent amplitudes with θ_u , θ_v and θ_p phases of the solutions, and W_0 is either 30 or 60. Note that each of the above amplitudes and phases of the solution is dependent upon both the coordinates R and Z . Solutions for the amplitude as well as the phases of the velocity components U and V and the excess entrance pressure P_1 are given in Tables I and II. As indicated in the tabulated results, the solution approaches the developed flow result with V and P_1 approaching zero for large values of Z , and the velocity profile approaches the entrance boundary condition given by equations (6) and (7) (where $A_u \rightarrow U_0(R)$, $\theta_u \rightarrow 0$ and $A_v \rightarrow 0$) as Z

Table I. Analytical solutions for amplitudes (A) and phases (θ) of the axial and radial velocity components and excess entrance pressure at $W_0 = 30$ and selected (R, Z) points. (All phase angles are given in degrees relative to that of the entrance flow velocity.)

Z	R	A_u	θ_u	A_v	θ_v	A_p	θ_p
0.000	0.000	1.05683	0.00	0.00000		5.65761	-164.92
0.000	0.975	0.75536	0.00	0.00544	0.11	60.24467	-1.73
0.020	0.000	1.00103	-0.04	0.00000		5.76113	-165.62
0.020	0.975	0.69869	0.08	0.06184	178.52	41.58482	-2.00
0.100	0.000	1.02046	-1.01	0.00000		4.61052	-164.17
0.100	0.975	0.39803	2.15	0.03606	175.63	11.20470	-2.07
0.400	0.000	1.19773	-9.85	0.00000		1.68158	-155.95
0.400	0.975	0.16994	20.76	0.00247	154.18	0.78742	34.00
0.600	0.000	1.29812	-14.51	0.00000		0.77756	-148.44
0.600	0.975	0.15754	26.89	0.00067	143.22	0.36511	56.63
1.200	0.000	1.38573	-18.59	0.00000		0.06755	-124.13
1.200	0.975	0.15421	29.67	0.00002	174.82	0.03591	65.97

Table II. Analytical solutions for amplitudes (A) and phases (θ) of the axial and radial velocity components and excess entrance pressure at $W_0=60$ and selected (R, Z) points. (All phase angles are given in degrees relative to that of the entrance flow velocity.)

Z	R	A_u	θ_u	A_v	θ_v	A_p	θ_p
0.000	0.000	1.0568	0.0	0.0000		6.6891	-157.2
0.000	0.975	0.7554	0.0	0.0054	0.2	59.4617	-2.1
0.020	0.000	1.0007	0.0	0.0000		6.7268	-158.4
0.020	0.975	0.6987	0.2	0.0619	177.0	40.8582	-2.2
0.100	0.000	1.0121	-0.6	0.0000		5.4079	-158.0
0.100	0.975	0.4018	4.1	0.0354	171.9	10.8589	0.7
0.400	0.000	1.0849	-6.8	0.0000		2.0649	-153.7
0.400	0.975	0.2097	27.2	0.0019	142.8	1.1751	36.7
0.600	0.000	1.1145	-10.2	0.0000		0.9893	-149.2
0.600	0.975	0.2046	31.2	0.0004	138.9	0.5232	42.2
1.000	0.000	1.1387	-12.6	0.0000		0.2038	-139.2
1.000	0.975	0.2025	32.4	0.0001	169.4	0.0941	45.8
1.200	0.000	1.1437	-12.8	0.0000		0.0902	-134.2
1.200	0.975	0.2021	32.5	0.0000	173.7	0.0396	50.4

approaches zero. Comparisons between the analytic solutions and the numerical solutions obtained with the finite element method are given later in Figures 1-3 for $W_0=30$.

FINITE ELEMENT APPROXIMATIONS AND RESULTS

Forming a weighted residual statement for the axisymmetric Stokes flow system in equations (1)-(3) and integrating by parts in the cylindrical geometry leads to a weak variational statement for the solution field (U, V, P): find (U, V, P) satisfying the essential boundary conditions (no slip on the wall and the inlet flow condition) together with the initial condition (no flow) and such that

$$\int_{\Omega} \left(\frac{\partial U}{\partial T} w_1 + \frac{\partial P}{\partial Z} w_1 + \frac{\partial U}{\partial R} \frac{\partial w_1}{\partial R} + \frac{\partial U}{\partial Z} \frac{\partial w_1}{\partial Z} \right) d\Omega = 0, \quad (24)$$

$$\int_{\Omega} \left(\frac{\partial V}{\partial T} w_2 + \frac{\partial P}{\partial R} w_2 + \frac{\partial V}{\partial R} \frac{\partial w_2}{\partial R} + \frac{\partial V}{\partial Z} \frac{\partial w_2}{\partial Z} + \frac{V w_2}{R^2} \right) d\Omega = 0, \quad (25)$$

$$\int_{\Omega} q \nabla \cdot \mathbf{u} d\Omega = 0 \quad (26)$$

for all admissible test functions (w_1, w_2, q). Since the problem is axisymmetric, no angular dependence enters in the formulation of the problem and the domain can be discretized using a two-dimensional section in the R - Z plane. Introducing a finite element discretization and associated piecewise polynomial bases, the velocity component and pressure expansions are given by

$$U^h(R, Z) = \sum_{j=1}^N U_j \Phi_j(R, Z), \quad (27)$$

$$V^h(R, Z) = \sum_{j=1}^N V_j \Phi_j(R, Z), \quad (28)$$

$$P^h(R, Z) = \sum_{j=1}^N P_j \Psi_j(R, Z). \quad (29)$$

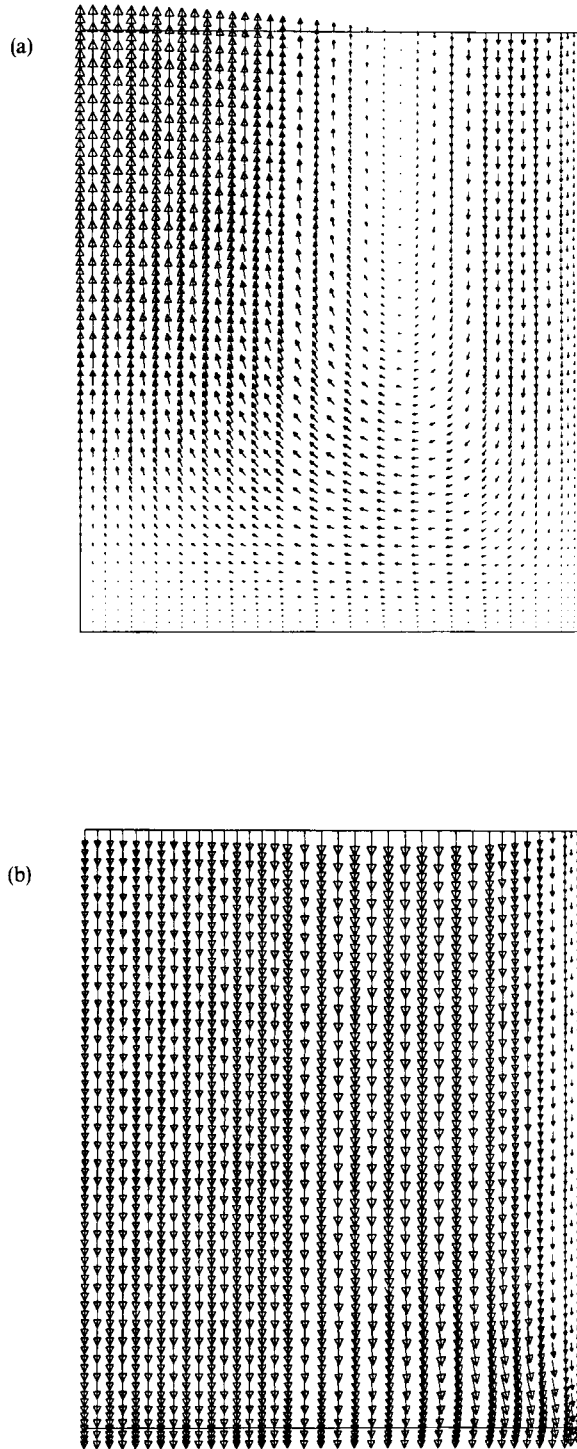


Figure 1. Velocity vector plots in (R, Z) section for inlet velocity $U_0(R) \cos(W_0 T)$ with (a) $W_0 T = \pi/2$, dimensionless maximum velocity 0.451 and (b) $W_0 T = 3\pi/4$, dimensionless maximum velocity 0.893

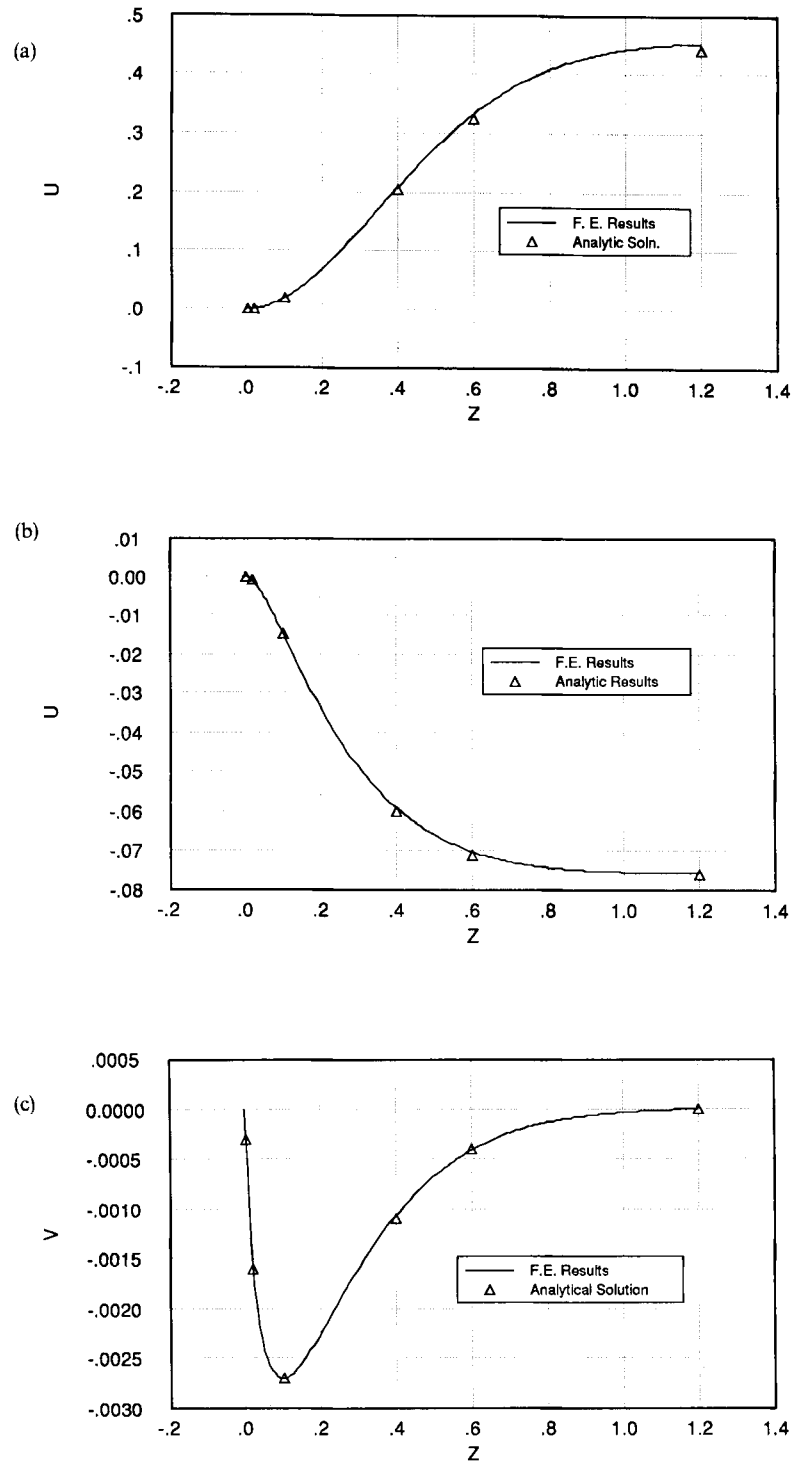


Figure 2. Comparisons of semi-analytical and finite element results for $W_0 T = \pi/2$: (a) U at $R=0$; (b) U at $R=0.975$; (c) V at $R=0.975$

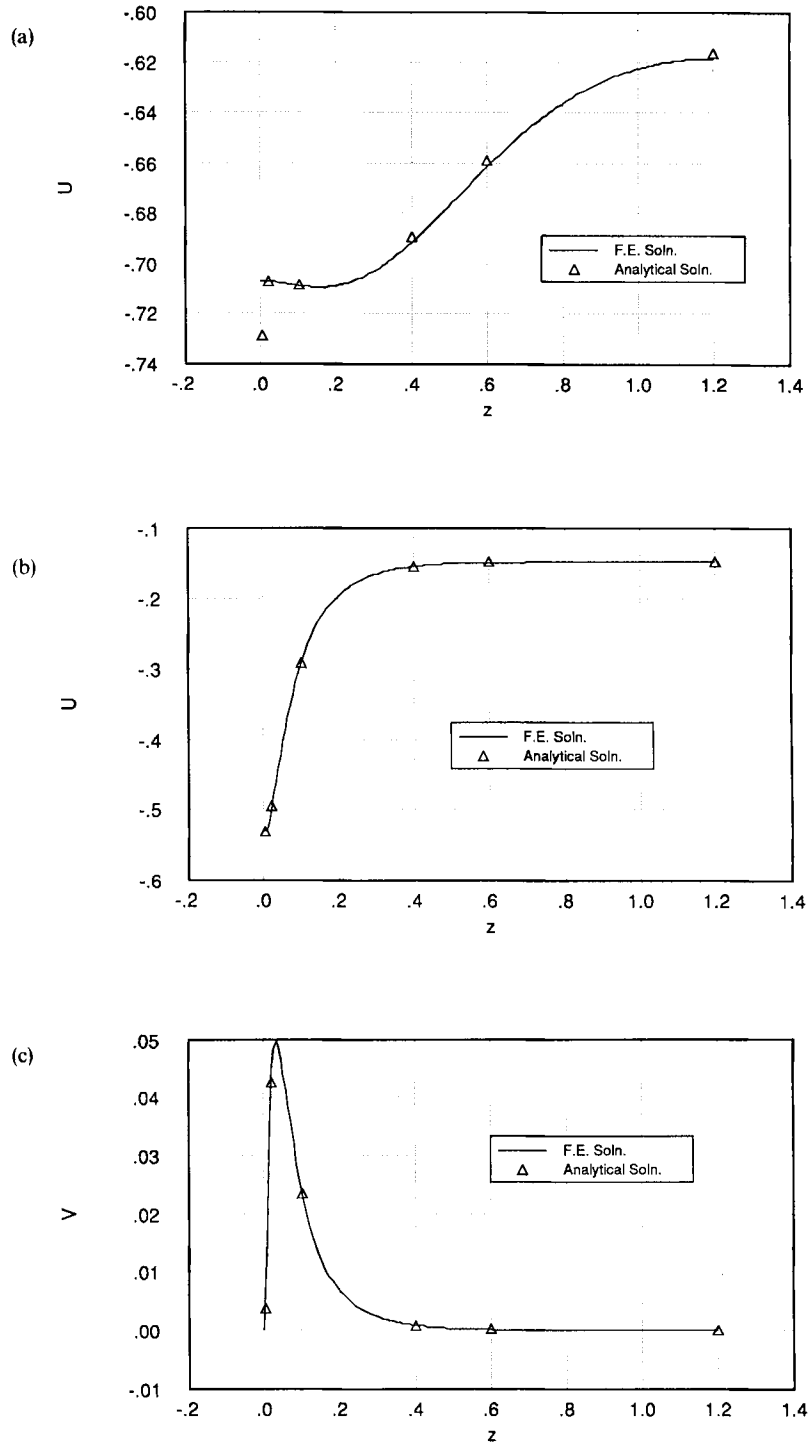


Figure 3. Comparisons of semi-analytical and finite element results for $W_0 T = 3\pi/4$: (a) U at $R=0$; (b) U at $R=0.975$; (c) V at $R=0.975$

Substituting into the previous weak integral statement, we obtain a semidiscrete system of ordinary differential equations of the form (see e.g., Carey and Oden⁷)

$$\mathbf{M} \begin{bmatrix} \dot{\mathbf{U}} \\ \dot{\mathbf{V}} \\ \dot{\mathbf{P}} \end{bmatrix} + \mathbf{K} \begin{bmatrix} \mathbf{U} \\ \mathbf{V} \\ \mathbf{P} \end{bmatrix} = \mathbf{0}. \quad (30)$$

This system is to be integrated with respect to time from the specified initial data. In the present calculations this system is integrated using an explicit-predictor/implicit-corrector scheme with time step chosen conservatively small to better assess the effect of spatial discretization.⁸ Of particular interest here are periodic flows, so the system (30) was accurately integrated through two inlet velocity cycles, by which point transient effects become negligible and the periodic state is attained. Numerical results at different times during an inlet cycle were examined. The computed finite element solution was started at $T = -\pi/2W_0$. This means that $W_0T = -\pi/2$ or that the inlet flow is zero and $\mathbf{u} = 0$ everywhere, thereby avoiding an ill-posed problem. Also from the semi-analytical solution we know that the cross-stream velocity V is essentially zero and the pressure is constant by $Z = 1.2$; therefore we set $V = 0$ and the normal stress to zero at $Z = 1.2$ as downstream boundary conditions with the discretized domain $0 < Z < 1.2$.

The finite element calculations were made on a graded 12×25 mesh in the (R, Z) frame using eight node velocity/four-node pressure C^0 quadrilateral elements. The mesh was fine near the wall and inlet regions. Velocity vector plots provide good flow field visualization and representative results are shown in Figure 1. The length of the arrows and size of the arrowheads are scaled linearly with the velocity magnitude. Since the velocity vectors are plotted from the element nodes, the distribution of velocity vectors corresponds also to the grading of the mesh. The two flow fields displayed correspond to inlet flow zero ($W_0T = \pi/2$) and later ($W_0T = 3\pi/4$) when the flow is directed outwards (in the reverse half-cycle). Note that when the inlet velocity is zero the periodic flow has a well-defined separation and reverse flow near the wall.

Using the analytical results for amplitude and phase in Table I, the velocity components are computed and compared in Figures 2 and 3 with the finite element results. The axial component U for $W_0T = \pi/2$ (Figure 1(a)) is graphed along the centreline ($R = 0$) and near the wall ($R = 0.975$) in Figures 2(a) and 2(b), demonstrating good agreement. The comparisons at $R = 0.4$ and 0.8 (not shown) were of similar quality. The radial velocity component V is also shown in Figure 2(c) at $R = 0.975$ and agreement is again good. Next the same sections are compared when the inlet velocity has decreased through the eighth period from zero (Figure 1(b)). The axial components are given in Figures 3(a) and 3(b) and the radial component in Figure 3(c). Note that in Figure 3(a) there is a slight discrepancy at $Z = 0$ due to the inability of the semi-analytic solution to match the inlet boundary condition with the number of modes utilized. At all other points agreement is good. For $W_0 = 60$ the morphology of the flow is the same and agreement between the two methods is the same as that shown in Figures 2 and 3 at $W_0 = 30$.

CONCLUSIONS

Semi-analytic solutions to the problem involving axisymmetric time-dependent periodic Stokes flow of a Newtonian fluid in the entrance region of a semi-infinite cylindrical tube are given. The resulting solutions are presented as a bench-mark for comparison with and evaluation of finite element Galerkin methods for the numerical solution to non-steady periodic Stokes flow problems. Comparisons between the semi-analytic solutions and the finite element solutions are presented along the centre of the tube ($R = 0$) and near the wall of the tube ($R = 0.975$).

ACKNOWLEDGEMENTS

This study has been supported in part by the Texas Advanced Technology Program and NIH Grant Number S14RR02721-04. We would like to express our appreciation to R. T. Folk for his suggestions and to the University of Texas System Center for High Performance Computing and St. Mary's University Computer Center.

REFERENCES

1. J. R. Womersley, 'An elastic tube theory of pulse transmission and oscillatory flow in mammalian arteries, *WADC Technical Report TR 56-614*, Wright Air Development Center, U.S. Air Force, 1957.
2. L. H. Benson and S. A. Trogdon, 'An eigenfunction solution for entry flow in a semi-infinite pipe at low Reynolds numbers', *Appl. Sci. Res.*, **42**, 347-359 (1985).
3. I. S. Goldberg and R. T. Folk, 'Solutions for steady and non-steady entrance flow in a semi-infinite circular tube at very low Reynolds numbers', *SIAM J. Appl. Math.*, **48**, 770-791 (1988).
4. H. B. Atabek and C. C. Chang, 'Oscillatory flow near the entry of a circular tube', *Z. Angew. Math. Phys.*, **12**, 185-201 (1961).
5. H. S. Lew and Y. C. Fung, 'On the low-Reynolds-number entry flow into a circular cylindrical tube', *J. Biomech.*, **2**, 105-119 (1969).
6. N. R. Kuchar and S. Ostrach, 'Unsteady entrance flow in elastic tubes with application to the vascular system', *Technical Report FTAS/TR67-25*, School of Engineering, Case Western Reserve University, Cleveland, OH, 1967.
7. G. F. Carey and J. T. Oden, *Finite Elements in Fluid Mechanics*, Prentice-Hall, Englewood Cliff, NJ, 1986.
8. P. M. Gresho, R. L. Lee and R. L. Sani, 'On the time dependent solution of incompressible Navier-Stokes equations in two and three dimensions', in *Recent Advances in Numerical Methods in Fluids, Vol. 1*, Pineridge Press, Swansea, 1980, pp. 27-81.